

## Cyclic Polymers from Alkynes: Scope and Degradation

Parker T. Boeck, Rinku Yadav, Brent S. Sumerlin,\* and Adam S. Veige\*



Cite This: *Macromolecules* 2024, 57, 71–77



Read Online

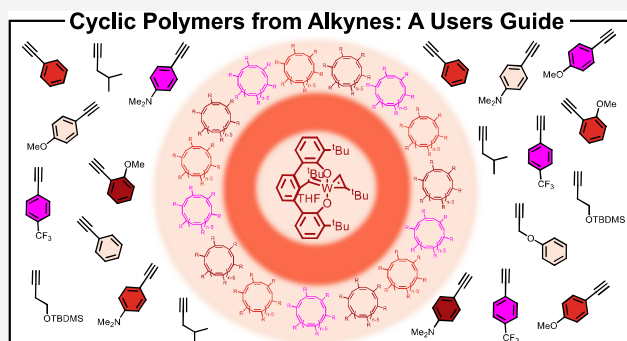
ACCESS |

Metrics & More

Article Recommendations

Supporting Information

**ABSTRACT:** Presented is the synthesis of cyclic polyacetylenes from alkynes and a study probing the functional group tolerance of catalyst **1**. The synthesized polymers were characterized by employing GPC, NMR, and IR spectroscopy. The cyclic polyacetylenes spontaneously degrade, leading to the formation of lower molecular weight linear analogues. The degradation rate varied significantly based on the monomer substituents. These discoveries collectively reveal the functional group limits of catalyst **1** and the subsequent stability of the synthesized polymers, thus opening new avenues for advanced polymer design and applications.



### INTRODUCTION

Energy storage,<sup>1</sup> sensors,<sup>2</sup> organic solar cells,<sup>3,4</sup> and organic field effect transistors<sup>5</sup> are all applications that utilize conjugated polymers. These applications take advantage of the unique electronic structure of extended  $\pi$ -conjugation.<sup>6</sup> In particular, substituted polyacetylenes are soluble analogues with interesting properties such as electrical conductivity and photoconductivity.<sup>7–14</sup> Additionally, the secondary structure of these macromolecules offers opportunities to expand their application space.<sup>15</sup> For example, enantiomer resolution<sup>16–19</sup> and chiral sensing<sup>20,21</sup> are two applications that take advantage of the helical nature of poly(phenylacetylene)s. Important for these applications, the properties of substituted polyacetylenes change by choice of alkyne monomer, and the resulting polymers are typically soluble, easily processed, and flexible.<sup>22</sup>

Cyclic polymers are topological isomers with no chain ends that exhibit different solution-state (radius of gyration,<sup>23–25</sup> intrinsic viscosity<sup>26,27</sup>) and solid-state (glass transition temperature<sup>28,29</sup>) properties than their linear analogues. Two general approaches to synthesize cyclic polymers include ring expansion of a metallacycle or monomer and ring closure of a linear polymeric precursor. The high dilution typically required to suppress bimolecular side reactions during ring closure generally prevents large-scale production of cyclic polymers via this method.<sup>30</sup> Moreover, ring expansion methodologies can yield much larger cyclic polymers ( $M_n = 100$ –1000 kDa) than ring closure.<sup>31,32</sup>

Catalyst **1** polymerizes alkynes to produce substituted *cyclic* polyacetylenes via ring expansion polymerization (REP) according to Figure 1.<sup>33</sup> It is now possible to examine the influence of a cyclic topology on all the interesting properties of substituted polyacetylenes. However, the monomer scope explored thus far is somewhat limited.<sup>30,34–37</sup> In this work,

catalyst **1** is tested for functional group tolerance and activity with a series of aliphatic and aromatic alkynes. The results indicate catalyst **1** is relatively functional-group-tolerant and successfully polymerizes a wide variety of electron-rich and electron-poor alkynes. Upon exposure to oxygen, the resulting polymers rapidly degrade into linear polymers in solution and demonstrate a dramatic functional group dependence on the rate of oxidative degradation.

### RESULTS AND DISCUSSION

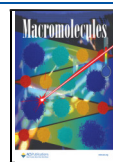
Polymerization initiates by combining a stock solution of **1** into a solution containing alkyne monomer under an inert atmosphere. The polymerization results in an immediate increase in viscosity and a concurrent color change. Upon precipitating the resultant cyclic polyacetylenes in degassed methanol and removing all volatiles under vacuum, a consistent high yield of these cyclic polyacetylenes can be achieved, typically exceeding 95%. Using gel permeation chromatography (GPC) with dimethylacetamide (DMAc) containing 50 mM LiCl as the eluent at 50 °C and static light scattering detection (Figures S1–S10), the absolute molecular weights of the synthesized polymers were determined. Alternatively, GPC was performed using THF as the eluent at 30 °C using static light scattering detection. Figure 1 depicts the outcome of the polymerizations and lists the various polymers synthesized in the study.

Received: September 28, 2023

Revised: November 23, 2023

Accepted: December 4, 2023

Published: December 19, 2023



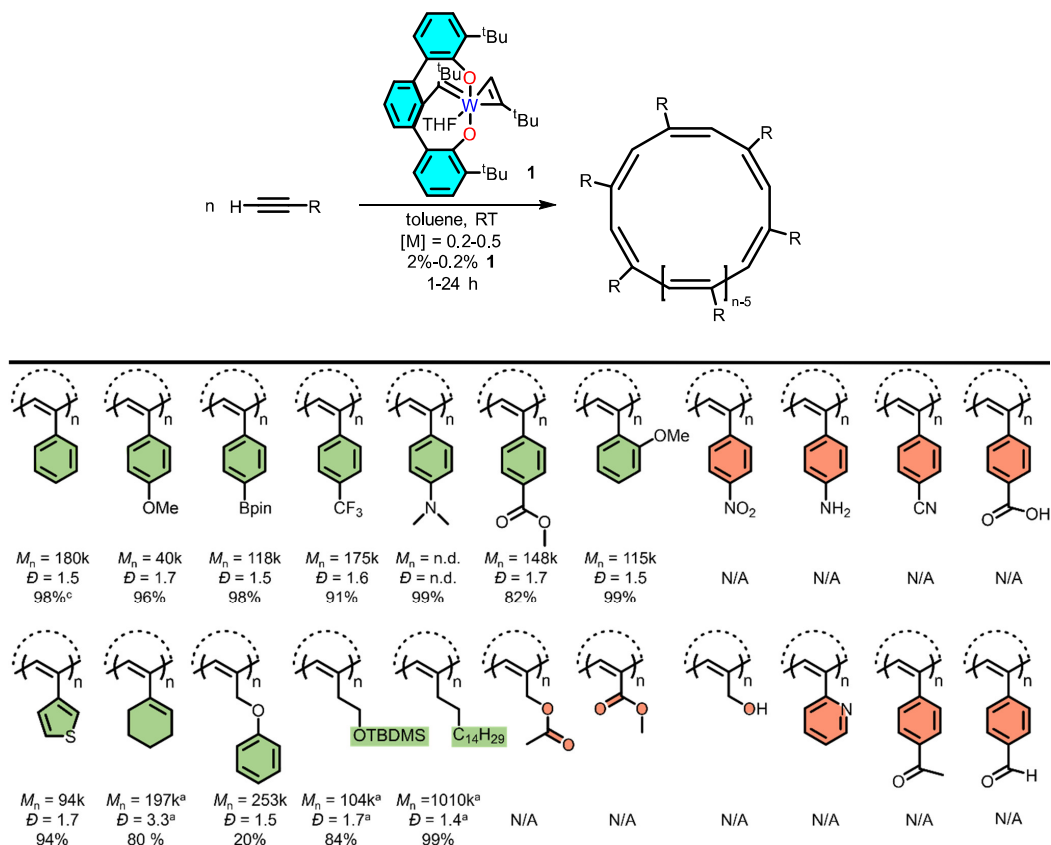


**Figure 1.** Catalyst **1** polymerization results with various alkynes. All polymers are drawn in the *trans* configuration for simplicity. Absolute molecular weight (g/mol) measured using GPC (DMAc, 50 °C, 50 mM LiCl) with a static light scattering detector (All molecular weights were measured using this system unless otherwise mentioned). <sup>a</sup>Absolute molecular weight measured using GPC (THF, 30 °C) with a static light scattering detector.

The results indicate catalyst **1** is not sensitive to the electronics of the alkyne. Phenylacetylene derivatives that bear electron-donating (NMe<sub>2</sub> and OMe) and electron-withdrawing (CF<sub>3</sub> and COOMe) groups in the *para*-position result in excellent yields and produce polymers with high molecular weights, consistently above 100 kg/mol. This aspect holds significance since other catalysts and polymerization methods are sensitive to the electronics of the monomers, requiring catalyst-monomer matching. It is important to note that due to its exceedingly rapid degradation upon dissolution in DMAc, the molecular weight of cyclic poly(4-ethynyl-*N,N*-dimethylaniline) (cPPA-NMe<sub>2</sub>) could not be determined.

Early transition metals,<sup>38–40</sup> particularly tungsten,<sup>41–43</sup> exhibit a notable affinity for oxygen (oxophilicity), so oxygen-containing alkyne monomers are challenging to polymerize. However, catalyst **1** successfully polymerizes the ester group-containing monomer methyl 4-ethynylbenzoate. Unfortunately, monomers such as propargyl acetate and ethyl propiolate, where the ester group is closer to the alkyne, did not polymerize. When the ester group is in proximity to the alkyne (as observed with propargyl acetate), it is possible that coordination occurs, impeding subsequent monomer addition. For methyl 4-ethynylbenzoate, the ester group remains distant from the active center during the polymerization. Monomers containing carbonyl groups are particularly poor substrates, but oxygen-containing phenyl propargyl ether and 2-ethynylanisole, where the ethers are near the alkyne, yield polymers with high molecular weights ( $M_n = 115k$  and  $252k$  g/mol,

respectively). Interestingly, 1-ethynyl-cyclohexene polymerizes without affecting the double bond, showcasing the remarkable selectivity of catalyst **1** in alkyne polymerization. <sup>1</sup>H NMR, <sup>13</sup>C NMR, and IR spectroscopy corroborate the structural characterization of all synthesized polyacetylenes (Figures S11–S40).

Even sterically hindered alkynes such as octadecyne and (but-3-yn-1-yloxy)(*tert*-butyl)dimethylsilane polymerize using catalyst **1**. The resultant polymer from octadecyne has a high molecular weight (>1000k g/mol) and lengthy side chains. As expected, monomers containing nucleophilic groups and relatively acidic protons, including propargyl alcohol and 4-ethynylaniline, do not polymerize. Monomers such as 4-ethynylbenzaldehyde, 4-(ethynylphenyl)ethenone, and 4-ethynylbenzoic acid did not polymerize either. Once again, the common factor among these nonpolymerizing monomers is the presence of a carbonyl functionality. This observation aligns with the anticipated oxophilicity of tungsten, which likely engenders coordination that obstructs initial or subsequent monomer coordination or complete O atom transfer to tungsten.<sup>41–44</sup>

Catalyst **1** polymerizes 3-ethynylthiophene to yield poly(3-ethynylthiophene) with a high molecular weight ( $M_n = 94k$  g/mol) and yield (94%). Nevertheless, polymerizing alkynes containing other heteroatoms capable of coordinating was not successful. For example, catalyst **1** does not polymerize 2-ethynylpyridine, even at a catalyst loading of 1:50. Again, coordination of pyridine to the tungsten center likely hinders

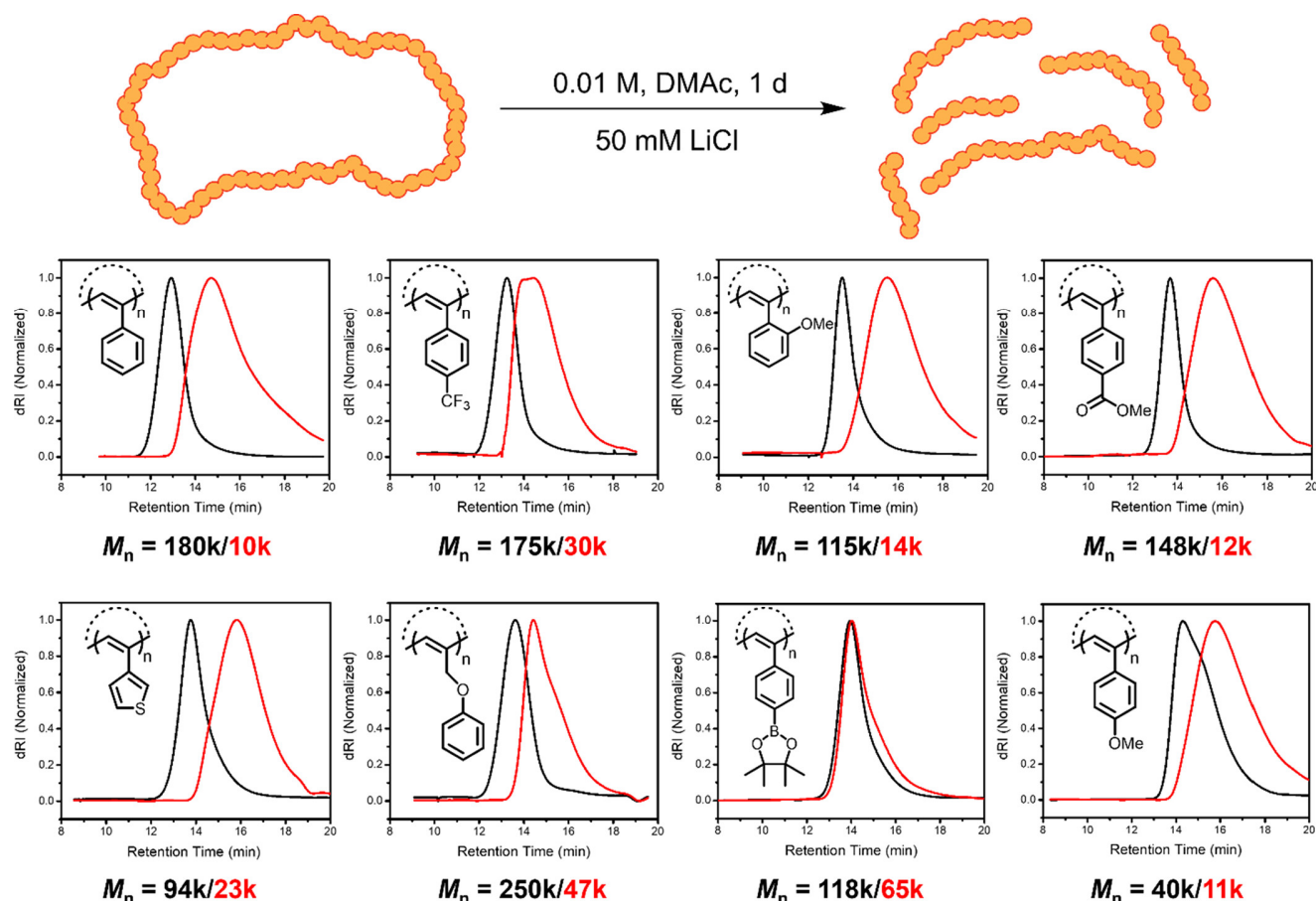


**Figure 2.** GPC chromatograms before (black) and after (red) dissolving the polymer in DMAc solvent for 1 d. Absolute number-average molecular weight was measured using GPC (DMAc, 50 °C, 50 mM LiCl) equipped with a static light scattering detector.

the polymerization. Attributable to coordination of nitrile and nitro groups to the metal center, catalyst 1 does not polymerize 4-ethynylbenzonitrile or 4-ethynylnitrobenzene. With a comprehensive understanding of the catalyst functional group tolerance achieved, the focus shifted to investigating the stereochemistry of the synthesized polymers.

Integrating the *cis*-alkene proton relative to the *trans*-alkene proton combined with the area of the underlying aromatic protons provides an approximate *cis* content for cyclic poly(phenylacetylene) (cPPA) by <sup>1</sup>H NMR spectroscopy.<sup>45</sup> Corroborating the NMR value is possible by examining the ratio of the absorptions at 760 and 740 cm<sup>-1</sup> in the IR spectrum of cPPA.<sup>46</sup> Both <sup>1</sup>H NMR and IR spectroscopy indicate cPPA synthesized with 1 contains a high percentage (~90%) of *cis*-double bonds (Figures S20 and S31). Poly(2-ethynylanisole) and poly(methyl 4-ethynylbenzoate) also have a high percentage of *cis*-double bonds (73 and 81%, respectively).<sup>45</sup> Unfortunately, the *cis*-content of polyacetylenes bearing alkyl substituents cannot be assessed using these methods. Next, the focus switched to determining the solution state stability of the synthesized polymers.

In a previous study, cyclic poly(4-methylpentyne) produced using catalyst 1 decomposed in the solid state upon extended exposure to air (18 h). However, the molecular weight and topology before and after were not analyzed.<sup>30</sup> When dissolved in DMAc (containing 50 mM LiCl), a common GPC eluent, all synthesized polyacetylenes spontaneously degrade at room temperature. Decomposition in a GPC solvent such as DMAc

has significant implications for characterizing polymers synthesized using catalyst 1, as cleavage of the cyclic polymer backbone leads to formation of lower molecular weight linear polymers. GPC instruments often have sample queues, potentially leading to degradation before analysis. To mitigate this concern, GPC analyses were performed immediately upon dissolution to minimize degradation.

Dissolving cPPA in solution initially reveals a narrow dispersity ( $D = 1.3$ ) and high molecular weight ( $M_n = 180\text{k g/mol}$ ). Reanalyzing the same sample 24 h later indicates a decrease in the  $M_n$  to 10k g/mol and an increase in dispersity to  $D = 2.4$ , unambiguously confirming polymer degradation. All the polymers degrade, with some experiencing an order of magnitude reduction in molecular weight in just 1 d (Figure 2).

Interestingly, cyclic poly(4-ethynylphenylboronic acid pinacolester) (cPPA-BPin) exhibits significantly suppressed degradation rates compared to other polymers.<sup>47</sup> The presence of the electron-withdrawing boronate ester clearly suppresses degradation. Conversely, cPPA-NMe<sub>2</sub> degrades rapidly, impeding accurate molecular weight assessment as it degrades prior to reaching the GPC detector (15 min). The tertiary amine within the polymer expedites degradation (Figure 3). Comparatively, cyclic poly(4-ethynylanisole), a poorer electron donor, correspondingly degrades more slowly than cPPA-NMe<sub>2</sub>, suggesting the donating capacity of the substituent accelerates the degradation rather than its Lewis base nature. Dissolving cyclic poly(phenylacetylene) in DMAc containing

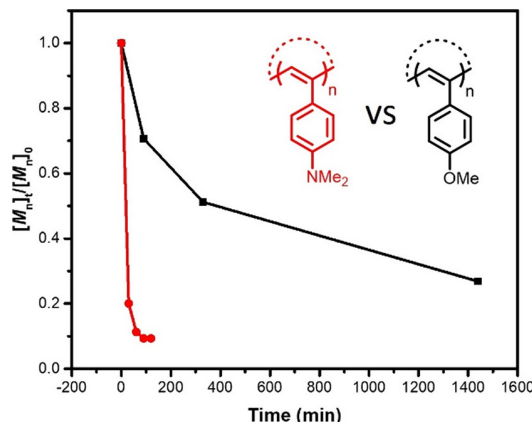


**Figure 3.** Normalized molecular weight loss over time upon dissolution in DMAc. Relative molecular weights were obtained using GPC (DMAc, 50 °C, 50 mM LiCl) against a calibration curve of PMMA standards.

one equiv of *N,N*-dimethylaniline or phenylboronic acid pinacol ester does not change the degradation rate (Figure S45), further confirming the Lewis acidity/basicity of the functional group is not responsible for altering the degradation rate difference between cPPA-NMe<sub>2</sub>, cPPA-BPin, and cPPA.

Presumably, backbone cleavage of a cyclic polymer results in a linear polymer, as illustrated in Figure 2. Linear polymers elute faster during GPC due to their larger hydrodynamic volume in solution compared to cyclic polymers of the same molecular weight.<sup>48,49</sup> Figure 4 depicts the log(molar mass)

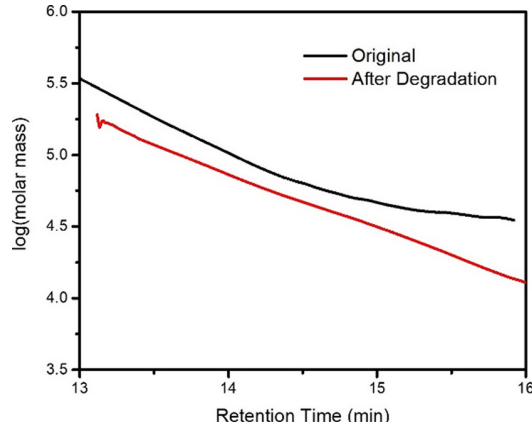


**Figure 4.** Log(molar mass) versus retention time plot for cPPA-CF<sub>3</sub> before (black) and after (red) dissolution in DMAc for 1 d measured using GPC (DMAc, 50 °C, 50 mM LiCl).

versus retention time of the same cyclic poly(1-ethynyl-4-(trifluoromethyl)benzene (cPPA-CF<sub>3</sub>) before and after degradation. The discernible shift in retention times at a given molecular weight before and after degradation corresponds to cyclic to linear polymer conversion. Furthermore, degradation leads to an increase in the root-mean-square radii of gyration of cPPA-CF<sub>3</sub> at the same molecular weight, consistent with a shift from cyclic to linear topology (Figure S50).<sup>50–52</sup> The change in hydrodynamic volume upon degradation is consistent across other polymers (Figures S51 and S52).

Cyclization<sup>53–55</sup> and oxidation<sup>56,57</sup> are two proposed mechanisms for the degradation of polyacetylenes. Monitoring

the degradation of cPPA-NMe<sub>2</sub> using <sup>1</sup>H NMR spectroscopy (CDCl<sub>3</sub>) and analyzing the subsequent polymer residues with IR spectroscopy provide insight into the mechanism. Notably, the formation of heptatriene and 1,3,5-benzene derivatives, consistent with electrocyclization-driven degradation, was conspicuously absent (Figure S54). Instead, the emergence of a singlet at 9.85 ppm (Figure S55), in line with aldehyde end group formation, unequivocally points to degradation occurring through the well-established<sup>56</sup> oxidative mechanism. Furthermore, an IR spectrum of the polymer residue obtained from evaporating the NMR solvent unveiled a carbonyl absorption at 1723 cm<sup>−1</sup>, corroborating the signature of oxidative degradation as depicted in Figure 5.<sup>56</sup> Oxidative degradation of phenylacetylenes occurs in a wide range of solvents including toluene, THF, CHCl<sub>3</sub>, and now DMAc.<sup>56</sup>

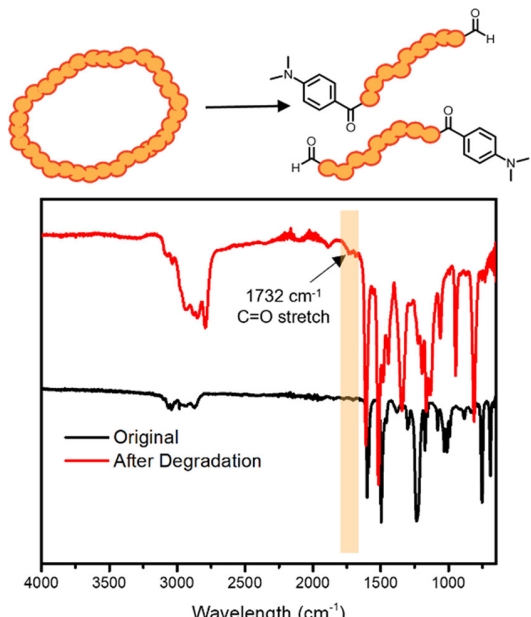


**Figure 5.** IR spectrum of cPPA-NMe<sub>2</sub> before and after degradation in CDCl<sub>3</sub>. The observation of carbonyl absorptions in the spectrum indicates an oxidative degradation mechanism.

During the oxidative degradation of cPPA-NMe<sub>2</sub> a color change from orange to green was observed. Monitoring the reaction via <sup>1</sup>H NMR spectroscopy (see Figure S54) reveals that the intensity of the resonance corresponding to the *cis*-backbone proton at 5.82 ppm decreases over the course of oxidative degradation, suggesting isomerization is occurring.<sup>46,58</sup> This raises the question of whether the color change is due to degradation or isomerization? To determine the origin of the color change cPPA-NMe<sub>2</sub> was dissolved in anhydrous and air-free CDCl<sub>3</sub> in a sealable NMR tube. Again, the intensity of the resonance at 5.82 ppm decreased over time, but no products associated with degradation (cyclization or oxidation) were observed (Figures S56 and S57). Thus, the *cis*-to-*trans* isomerization of the backbone is responsible for the color change.

## CONCLUSIONS

A variety of aliphatic and aromatic alkynes were screened for reactivity with catalyst 1, and the solution state stability of the synthesized polymers was examined. Tolerated monomers

include aromatic alkynes, bearing both electron-donating and withdrawing groups, and aliphatic alkynes, including sterically hindered alkynes such as octadecyne. In contrast, monomers bearing strongly coordinating groups (pyridyl), acidic protons, and carbonyl functionalities did not polymerize. High yields (>95%) and high molecular weight (>100k g/mol) polymers form from monomers successfully polymerized by 1. Collectively, these discoveries improve our understanding of the substrate scope of catalyst 1 and help facilitate monomer design, thus ensuring successful polymerization.

The synthesized polyacetylenes spontaneously degrade into lower molecular weight linear polymers upon dissolution in DMAc. Ironically, this suggests *cyclic* polymers can act as precursors to previously inaccessible *linear* polymers. For example, degrading cyclic poly((but-3-yn-1-yloxy)(*tert*-butyl)-dimethylsilane) provides the previously inaccessible linear derivative. The rate of degradation was significantly impacted by the identity of the substituent, where electron-withdrawing groups (Bpin) retard degradation and electron-donating groups (NMe<sub>2</sub>) accelerate the degradation. The substituent effects are consistent with the proposed oxidative degradation. Strongly donating substituents raise the energy of the highest occupied molecular orbitals (HOMO). In the case of polyacetylenes the HOMO is the  $\pi$ -conjugated double bonds. Thus, raising the energy level of the conjugated double bonds facilitates reaction with oxygen leading to faster rates of degradation. The opposite is true for electron-withdrawing substituents, as observed in the case of cPPA-BPin. The difference in degradation rates suggests intriguing avenues for tailoring polymer stability. For example, it is reasonable to assume that a copolymer containing both PA-Bpin and phenylacetylene would undergo oxidative degradation much slower than a phenylacetylene homopolymer.

Finally, evidence of end-group carbonyls indicates oxidation is the active mechanism of degradation. A thorough understanding of this phenomenon greatly increases the reproducibility of polymer characterization going forward, allowing the user to minimize and/or prevent degradation prior to characterization. Discovered in this work, the stark contrast between the stability of polymers containing electron donating/withdrawing groups indicates future applications where users can tailor polymer stability. Insight into the oxidative degradation now enables the synthesis of both linear and cyclic polymers using catalyst 1.

## ASSOCIATED CONTENT

### Supporting Information

The Supporting Information is available free of charge at <https://pubs.acs.org/doi/10.1021/acs.macromol.3c01994>.

Full experimental procedures, NMR spectra, IR spectra, and GPC data ([PDF](#))

## AUTHOR INFORMATION

### Corresponding Authors

Brent S. Sumerlin – *George and Josephine Butler Polymer Research Laboratory, Center for Macromolecular Sciences and Engineering, Department of Chemistry, University of Florida, Gainesville, Florida 32611, United States;*  
[orcid.org/0000-0001-5749-5444](https://orcid.org/0000-0001-5749-5444); Email: [sumerlin@chem.ufl.edu](mailto:sumerlin@chem.ufl.edu)

Adam S. Veige – *Center for Catalysis, Department of Chemistry and George and Josephine Butler Polymer*

*Research Laboratory, Center for Macromolecular Sciences and Engineering, Department of Chemistry, University of Florida, Gainesville, Florida 32611, United States;*  
[orcid.org/0000-0002-7020-9251](https://orcid.org/0000-0002-7020-9251); Email: [veige@chem.ufl.edu](mailto:veige@chem.ufl.edu)

### Authors

Parker T. Boeck – *Center for Catalysis, Department of Chemistry and George and Josephine Butler Polymer Research Laboratory, Center for Macromolecular Sciences and Engineering, Department of Chemistry, University of Florida, Gainesville, Florida 32611, United States*  
Rinku Yadav – *Center for Catalysis, Department of Chemistry, University of Florida, Gainesville, Florida 32611, United States*

Complete contact information is available at:  
<https://pubs.acs.org/10.1021/acs.macromol.3c01994>

### Author Contributions

P.T.B. and R.Y. conceptualized the study and performed the polymerizations. P.T.B. collected, interpreted, and curated the data. P.T.B. performed degradation experiments and drafted the manuscript. P.T.B., R.Y., B.S.S., and A.S.V. revised the manuscript. A.S.V. and B.S.S. supervised the work.

### Notes

The authors declare the following competing financial interest(s): ASV, BSS, and UF are named inventors on patents filed on aspects of the catalyst and polymers.

## ACKNOWLEDGMENTS

This material is based upon work supported by the National Science Foundation, CHE-2108266. ASV, BSS, and UF are named inventors on patents filed on aspects of the catalyst and polymers.

## REFERENCES

- (1) Ren, J.; Wang, X.; Liu, H.; Hu, Y.; Zhang, X.; Masuda, T. Poly(Phenylacetylene)s Bearing Thianthrene Groups as High-Voltage Organic Cathode Materials for Lithium Batteries. *React. Funct. Polym.* **2020**, *146*, No. 104365.
- (2) Stewart, K.; Limbu, S.; Nightingale, J.; Pagano, K.; Park, B.; Hong, S.; Lee, K.; Kwon, S.; Kim, J. S. Molecular Understanding of a  $\pi$ -Conjugated Polymer/Solid-State Ionic Liquid Complex as a Highly Sensitive and Selective Gas Sensor. *J. Mater. Chem. C* **2020**, *8*, 15268–15276.
- (3) Price, S. C.; Stuart, A. C.; Yang, L.; Zhou, H.; You, W. Fluorine Substituted Conjugated Polymer of Medium Band Gap Yields 7% Efficiency in Polymer-Fullerene Solar Cells. *J. Am. Chem. Soc.* **2011**, *133*, 4625–4631.
- (4) Neu, J.; Samson, S.; Ding, K.; Rech, J. J.; Ade, H.; You, W. Oligo(Ethylene Glycol) Side Chain Architecture Enables Alcohol-Processable Conjugated Polymers for Organic Solar Cells. *Macromolecules* **2023**, *56*, 2092–2103.
- (5) Horowitz, B. G. Organic Field-Effect Transistors. *Adv. Mater.* **1998**, *5*, 365–377.
- (6) Namsheer, K.; Rout, C. S. Conducting Polymers: A Comprehensive Review on Recent Advances in Synthesis, Properties and Applications. *RSC Adv.* **2021**, *11*, S659–S697.
- (7) Tang, B. Z.; Chen, H. Z.; Xu, R. S.; Lam, J. W. Y.; Cheuk, K. K. L.; Wong, H. N. C.; Wang, M. Structure-Property Relationships for Photoconduction in Substituted Polyacetylenes. *Chem. Mater.* **2000**, *12*, 213–221.
- (8) Kang, E. T.; Ehrlich, P.; Bhatt, A. P.; Anderson, W. A. Charge Carrier Generation, Transport, and Trapping in a Photoconductive

Conjugated Polymer: Polyphenylacetylene. *Appl. Phys. Lett.* **1982**, *41*, 1136–1138.

(9) Kang, E. T.; Ehrlich, P.; Bhatt, A. P.; Anderson, W. A. Photoconductivity in Trans-Poly(Phenylacetylene) and Its Charge-Transfer Complexes. *Macromolecules* **1984**, *17*, 1020–1024.

(10) Zhao, J.; Yang, M.; Shen, Z. High Photosensitivity in Cis-Poly(Phenylacetylene) Films Irradiated by Electron Beams. *Polym. J.* **1991**, *23*, 963–968.

(11) Kang, E. T.; Neoh, K. G.; Masuda, T.; Higashimura, T.; Yamamoto, M. Photoconductivity in Poly[[o-(Trimethylsilyl)-Phenyl]Acetylene]. *Polymer* **1989**, *30*, 1328–1331.

(12) Xu, H. P.; Xie, B. Y.; Yuan, W. Z.; Sun, J. Z.; Yang, F.; Dong, Y. Q.; Qin, A.; Zhang, S.; Wang, M.; Tang, B. Z. Hybridization of Thiol-Functionalized Poly(Phenylacetylene) with Cadmium Sulfide Nano-rods: Improved Miscibility and Enhanced Photoconductivity. *Chem. Commun.* **2007**, 1322–1324.

(13) Liu, X. Q.; Li, Y. L.; Lin, Y. W.; Yang, S.; Guo, X. F.; Li, Y.; Yang, J.; Chen, E. Q. Composites of Functional Poly(Phenylacetylene)s and Single-Walled Carbon Nanotubes: Preparation, Dispersion, and near Infrared Photoresponsive Properties. *Macromolecules* **2013**, *46*, 8479–8487.

(14) Kang, E. T.; Ehrlich, P.; Anderson, W. A. Semiconducting Photoconductors From Amorphous Films of Dye-Sensitized Polyphenylacetylene. *Mol. Cryst. Liq. Cryst.* **1984**, *106*, 305–316.

(15) Rodríguez, R.; Quiñoá, E.; Riguera, R.; Freire, F. Architecture of Chiral Poly(Phenylacetylene)s: From Compressed/Highly Dynamic to Stretched/Quasi-Static Helices. *J. Am. Chem. Soc.* **2016**, *138*, 9620–9628.

(16) Shi, G.; Dai, X.; Xu, Q.; Shen, J.; Wan, X. Enantioseparation by High-Performance Liquid Chromatography on Proline-Derived Helical Polyacetylenes. *Polym. Chem.* **2021**, *12*, 242–253.

(17) Zhang, C.; Wang, H.; Geng, Q.; Yang, T.; Liu, L.; Sakai, R.; Satoh, T.; Kakuchi, T.; Okamoto, Y. Synthesis of Helical Poly(Phenylacetylene)s with Amide Linkage Bearing L-Phenylalanine and L-Phenylglycine Ethyl Ester Pendants and Their Applications as Chiral Stationary Phases for HPLC. *Macromolecules* **2013**, *46*, 8406–8415.

(18) Shimomura, K.; Ikai, T.; Kanoh, S.; Yashima, E.; Maeda, K. Switchable Enantioseparation Based on Macromolecular Memory of a Helical Polyacetylene in the Solid State. *Nat. Chem.* **2014**, *6*, 429–434.

(19) Hirose, D.; Isobe, A.; Quiñoá, E.; Freire, F.; Maeda, K. Three-State Switchable Chiral Stationary Phase Based on Helicity Control of an Optically Active Poly(Phenylacetylene) Derivative by Using Metal Cations in the Solid State. *J. Am. Chem. Soc.* **2019**, *141*, 8592–8598.

(20) Anger, E.; Iida, H.; Yamaguchi, T.; Hayashi, K.; Kumano, D.; Crassous, J.; Vanthuyne, N.; Roussel, C.; Yashima, E. Synthesis and Chiral Recognition Ability of Helical Polyacetylenes Bearing Helicene Pendants. *Polym. Chem.* **2014**, *5*, 4909–4914.

(21) Zou, H.; Wu, Q. L.; Zhou, L.; Hou, X. H.; Liu, N.; Wu, Z. Q. Chiral Recognition and Resolution Based on Helical Polymers. *Chin. J. Polym. Sci.* **2021**, *39*, 1521–1527.

(22) Liu, J.; Lam, J. W. Y.; Tang, B. Z. Acetylenic Polymers: Syntheses, Structures, and Functions. *Chem. Rev.* **2009**, *109*, 5799–5867.

(23) Cassa, E. F. Some Statistical Properties of Flexible Ring Polymers. *J. Polym. Sci., Part A: Polym. Chem.* **1965**, *3*, 605–614.

(24) Roovers, J. Dilute-Solution Properties of Ring Polystyrenes. *J. Polym. Sci. Polym. Phys. Ed.* **1985**, *23*, 1117–1126.

(25) Gartner, T. E.; Haque, F. M.; Gomi, A. M.; Grayson, S. M.; Hore, M. J. A.; Jayaraman, A. Scaling Exponent and Effective Interactions in Linear and Cyclic Polymer Solutions: Theory, Simulations, and Experiments. *Macromolecules* **2019**, *52*, 4579–4589.

(26) Uhlík, F.; Roovers, J. Intrinsic Viscosity of Cyclic Polystyrene. *Macromolecules* **2017**, *50*, 7770–7776.

(27) Clarson, S. J.; Semlyen, J. A. Cyclic Polysiloxanes: 1. Preparation and Characterization of Poly(Phenylmethylsiloxane). *Polymer* **1986**, *27*, 1633–1636.

(28) Nam, S.; Leisen, J.; Breedveld, V.; Beckham, H. W. Dynamics of Unentangled Cyclic and Linear Poly(Oxyethylene) Melts. *Polymer* **2008**, *49*, 5467–5473.

(29) Clarson, S. J.; Dodgson, K.; Semlyen, J. A. Studies of Cyclic and Linear Poly(Dimethylsiloxanes): 19. Glass Transition Temperatures and Crystallization Behaviour. *Polymer* **1985**, *26*, 930–934.

(30) Miao, Z.; Pal, D.; Niu, W.; Kubo, T.; Sumerlin, B. S.; Veige, A. S. Cyclic Poly(4-Methyl-1-Pentene): Efficient Catalytic Synthesis of a Transparent Cyclic Polymer. *Macromolecules* **2020**, *53*, 7774–7782.

(31) Boydston, A. J.; Xia, Y.; Kornfield, J. A.; Gorodetskaya, I. A.; Grubbs, R. H. Cyclic Ruthenium-Alkylidene Catalysts for Ring-Expansion Metathesis Polymerization. *J. Am. Chem. Soc.* **2008**, *130*, 12775–12782.

(32) Wang, T. W.; Huang, P. R.; Chow, J. L.; Kaminsky, W.; Golder, M. R. A Cyclic Ruthenium Benzyldiene Initiator Platform Enhances Reactivity for Ring-Expansion Metathesis Polymerization. *J. Am. Chem. Soc.* **2021**, *143*, 7314–7319.

(33) Roland, C. D.; Li, H.; Abboud, K. A.; Wagener, K. B.; Veige, A. S. Cyclic Polymers from Alkynes. *Nat. Chem.* **2016**, *8*, 791–796.

(34) Miao, Z.; Kubo, T.; Pal, D.; Sumerlin, B. S.; Veige, A. S. PH-Responsive Water-Soluble Cyclic Polymer. *Macromolecules* **2019**, *52*, 6260–6265.

(35) Pal, D.; Miao, Z.; Garrison, J. B.; Veige, A. S.; Sumerlin, B. S. Ultra-High-Molecular-Weight Macrocyclic Bottlebrushes via Post-Polymerization Modification of a Cyclic Polymer. *Macromolecules* **2020**, *53*, 9717–9724.

(36) Miao, Z.; Gonsales, S. A.; Ehm, C.; Mentink-Vigier, F.; Bowers, C. R.; Sumerlin, B. S.; Veige, A. S. Cyclic Polyacetylene. *Nat. Chem.* **2021**, *13*, 792–799.

(37) Niu, W.; Gonsales, S. A.; Kubo, T.; Bentz, K. C.; Pal, D.; Savin, D. A.; Sumerlin, B. S.; Veige, A. S. Polypropylene: Now Available without Chain Ends. *Chem.* **2019**, *5*, 237–244.

(38) Schrock, R. R. The Reaction of Niobium and Tantalum Neopentylidene Complexes with the Carbonyl Function. *J. Am. Chem. Soc.* **1976**, *98*, 5399–5400.

(39) Wesendrup, R.; Schwarz, H. Tantalum-Mediated Coupling of Methane and Carbon Dioxide in the Gas Phase. *Angew. Chem., Int. Ed.* **1995**, *34*, 2033–2035.

(40) Sandig, N.; Koch, W. A Quantum Chemical View on the Mechanism of the Ta+-Mediated Coupling of Carbon Dioxide with Methane. *Organometallics* **1998**, *17*, 2344–2351.

(41) Fischer, E. O.; Filippou, A. C.; Alt, H. G.; Thewalt, U. Synthesis of  $[\text{Et}_2\text{N}-\text{C}\equiv\text{W}(\text{CO})_2(\mu-\text{PPh}_3)_2\text{Mo}(\text{CO})_4]$ , the First Anionic Carbyne metal Complex; Addition of  $\text{CO}_2$  to the  $\text{W}\equiv\text{C}$  Bond. *Angew. Chem., Int. Ed.* **1985**, *96*, 203–205.

(42) Gonsales, S. A.; Pascualini, M. E.; Ghiviriga, I.; Abboud, K. A.; Veige, A. S. Fast “Wittig-Like” Reactions As a Consequence of the Inorganic Enamine Effect. *J. Am. Chem. Soc.* **2015**, *137*, 4840–4845.

(43) Gonsales, S. A.; Ghiviriga, I.; Abboud, K. A.; Veige, A. S. Carbon Dioxide Cleavage across a Tungsten-Alkylidene Bearing a Trianionic Pincer-Type Ligand. *Dalt. Trans.* **2016**, *45*, 15783–15785.

(44) Gonsales, S. A.; Kubo, T.; Flint, M. K.; Abboud, K. A.; Sumerlin, B. S.; Veige, A. S. Highly Tactic Cyclic Polynorbornene: Stereoselective Ring Expansion Metathesis Polymerization of Norbornene Catalyzed by a New Tethered Tungsten-Alkylidene Catalyst. *J. Am. Chem. Soc.* **2016**, *138*, 4996–4999.

(45) Tang, B. Z.; Poon, W. H.; Leung, S. M.; Leung, W. H.; Peng, H. Synthesis of Stereoregular Poly(Phenylacetylene)s by Organorhodium Complexes in Aqueous Media. *Macromolecules* **1997**, *30*, 2209–2212.

(46) Simionescu, C. I.; Percec, V.; Dumitrescu, S. Polymerization of Acetylenic Derivatives. *J. Polym. Sci. Polym. Chem. Ed.* **1977**, *15*, 2497–2509.

(47) Debabrata, K.; Jakhar, V. K.; Stewart, K. A.; Lester, D. W.; Veige, A. S.; Sumerlin, B. S. Functionalized Cyclic Polymers and Network Gels. *Macromolecules* **2023**, submitted.

(48) Roovers, J.; Toporowski, P. M. Synthesis of High Molecular Weight Ring Polystyrenes. *Macromolecules* **1983**, *16*, 843–849.

(49) Laurent, B. A.; Grayson, S. M. Synthetic Approaches for the Preparation of Cyclic Polymers. *Chem. Soc. Rev.* **2009**, *38*, 2202–2213.

(50) Hoskins, J. N.; Grayson, S. M. Cyclic Polyesters: Synthetic Approaches and Potential Applications. *Polym. Chem.* **2011**, *2*, 289–299.

(51) Rubio, A. M.; Freire, J. J.; Complutense, U.; Bishop, M.; Clarke, J. H. R.  $\Theta$  State Transition Curves, and Conformational Properties of Cyclic Chains. *Macromolecules* **1995**, *28*, 2240–2246.

(52) Zimm, B. H.; Stockmayer, W. H. The Dimensions of Chain Molecules Containing Branches and Rings. *J. Chem. Phys.* **1949**, *17*, 1301–1314.

(53) Percec, V.; Rudick, J. G. Independent Electrocyclization and Oxidative Chain Cleavage along the Backbone of Cis-Poly(Phenylacetylene). *Macromolecules* **2005**, *38*, 7241–7250.

(54) Percec, V.; Rudick, J. G.; Nombel, P.; Buchowicz, W. Dramatic Decrease of the Cis Content and Molecular Weight of Cis-Transoidal Polyphenylacetylene at 23 °C in Solutions Prepared in Air. *J. Polym. Sci. Part A Polym. Chem.* **2002**, *40*, 3212–3220.

(55) Kong, X.; Wing, J.; Lam, Y.; Tang, B. Z. Synthesis, Mesomorphism, Isomerization, and Aromatization of Stereoregular Poly{[4-((6-((4'-Heptyl)Oxy-4-Biphenyl)Carbonyl)oxy)-Hexyl]Oxy}carbonyl]Phenyl]Acetylene}. *Macromolecules* **1999**, *32*, 1722–1730.

(56) Karim, S. M. A.; Nomura, R.; Masuda, T. Degradation Behavior of Stereoregular Cis–Transoidal Poly(Phenylacetylene)S. *J. Polym. Sci., Part A: Polym. Chem.* **2001**, *39*, 3130–3136.

(57) Vohlidal, J.; Redrova, D.; Pacovska, M.; Sedlacek, J. Autoxidative Degradation of Poly(Phenylacetylene). *Collect. Czechoslov. Chem. Commun.* **1993**, *58*, 2651–2662.

(58) Simionescu, C. I.; Percec, V.; Poni, P. Thermal Cis-Trans Isomerization of Cis-Transoidal Polyphenylacetylene. *J. Polym. Sci.: Polym. Chem. Ed.* **1980**, *18*, 147–155.